

1 **Preparation and characterization of natural rubber composites highly filled with**  
2 **brewers' spent grain/ground tire rubber hybrid reinforcement**

3  
4 Łukasz Zedler<sup>a</sup>, Xavier Colom<sup>b</sup>, Mohammad Reza Saeb<sup>c</sup>, Krzysztof Formela<sup>a\*</sup>

5  
6 <sup>a</sup>Department of Polymer Technology, Faculty of Chemistry, G. Narutowicza Str. 11/12,  
7 Gdańsk University of Technology, 80-233 Gdansk, Poland

8 <sup>b</sup>Universitat Politècnica de Catalunya Barcelona Tech, Department of Chemical  
9 Engineering, Colom 1, 08222-Terrassa, Barcelona, Spain

10 <sup>c</sup>Department of Resin and Additives, Institute for Color Science and Technology, P.O.  
11 Box: 16765-654, Teheran, Iran

12 \*Corresponding author: Krzysztof Formela, e-mail: [krzysztof.formela@pg.gda.pl](mailto:krzysztof.formela@pg.gda.pl) ,  
13 [kformela.ktp@gmail.com](mailto:kformela.ktp@gmail.com) , Tel. No.: +48 58 347 2234/ Fax. No.: +48 58 347 2134

14 **Abstract**

15 Brewers' spent grain (BSG) and ground tire rubber (GTR) were applied as low-cost  
16 hybrid reinforcement natural rubber (NR). The impact of BSG/GTR ratio (in range:  
17 100/0, 75/25, 50/50, 25/75 and 0/100 phr) on processing and performance properties of  
18 highly filled natural rubber composites was evaluated by oscillating disc rheometer,  
19 Fourier-transform infrared spectroscopy, thermogravimetric analysis, scanning electron  
20 microscopy, swelling behavior, tensile tests and impedance tube measurements. It was  
21 found that increasing content of GTR in NR/BSG/GTR composites accelerate cross-  
22 linking reactions during their preparation, which resulted in decrease of scorch time and  
23 optimal cure time. Simultaneously, higher content of GTR filler in NR/BSG/GTR  
24 composites significantly improved their physico-mechanical, thermal, morphological  
25 and acoustical properties. This indicates better compatibility between natural rubber  
26 matrix and GTR than with BSG, which is related to correlation between two factors.  
27 First factor is obvious differences in particles size and polarity of GTR and BSG, which  
28 affected physical interactions into phase boundary between NR matrix and BSG/GTR  
29 hybrid reinforcement. Second factor is possible migration of unreacted curing additives  
30 and carbon black particle from GTR filler to NR matrix, which played a significant role  
31 on processing and final properties of NR/BSG/GTR composites.

32  
33 **Keywords:** Brewers' spent grain; Ground tire rubber; Natural rubber; Biocomposites;  
34 Structure-property relationships

## 1           **1.Introduction**

2           Continuous increasing amount of industrial and agricultural wastes or by-  
3 products is a huge environmental issue all over the world. This unfavorable trend  
4 enforced the industry and scientific community to search and develop of  
5 environmentally-friendly and economical technologies their utilization [1-3].

6           Among many recycling methods, a very promising route to resolve waste  
7 utilization problem is the application of post-production and post-consumption wastes  
8 as filler/reinforcement in variable polymers (or their blends) to prepare novel materials  
9 with unique performance properties and/or reduce their final cost. In this field of  
10 research, using of lignocellulosic agriculture wastes as reinforcing phase in  
11 biocomposites gained more attention over the last two decades [4-6]. This is due to low  
12 cost, low density, good mechanical properties, renewability, abundance and  
13 biodegradability of lignocellulosic fillers, which affected increasing demand on  
14 biocomposites in a different branch of industry. However, weak compatibility between  
15 hydrophobic polymers and hydrophilic lignocellulosic fillers causes insufficient stress  
16 transfer to the reinforcing phase and consequently part failure at the matrix-  
17 lignocellulosic filler interface [7, 8]. This results in poor mechanical properties of  
18 prepared biocomposites, which is particularly observed in highly-filled composite  
19 materials. Therefore, many compatibilization strategies to improve matrix-  
20 lignocellulosic filler interfacial interactions, such as physical and chemical modification  
21 of polymer matrix, lignocellulosic fillers/fibers functionalization or reactive extrusion of  
22 biocomposites, have been investigated. Recent developments in this area were  
23 comprehensively described in works [9-11]. A relatively new strategy to improve  
24 performance properties of biocomposites is the application of hybrid fillers [12-14].  
25 Term “hybrid filler system” can be defined as a mixture of two (or more) fillers, which  
26 indicated synergistic effects superior than the sum of the effects for the individual filler  
27 [15].

28           In the present study, two kinds of wastes: i) brewers’ spent grain – BSG (a major  
29 by-product of brewing industry) and ii) ground tire rubber – GTR (disintegrated worn  
30 tires) were used. BSG filler contains mostly from cellulose, hemi-cellulose or lignin,  
31 while GTR filler is composed of natural rubber, synthetic rubbers, reinforcing fillers  
32 (carbon black or silica) and other additives (e.g. sulfur curing system, plasticizers,

1 antioxidants, etc.). From the economical and environmental point of view, GTR is  
2 a promising modifier of polymer composites reinforced with lignocellulosic fillers or  
3 fibers. The possible application of GTR in polypropylene/cellulosic filler composites  
4 [16, 17] and polyethylene/cellulosic filler composites [18-20] was extensively examined  
5 by Prof. Rodrigue research group from Université Laval Quebec City in Canada. It was  
6 found that incorporation of GTR in thermoplastics/cellulosic filler composites  
7 significantly enhanced impact strength, while simultaneously tensile properties  
8 deterioration was usually observed.

9 In our previous research [21] BSG/GTR hybrid filler was applied in  
10 polyurethane composites. The obtained results showed that processing and performance  
11 properties of obtained composites can be easily modified using variable BSG/GTR  
12 hybrid filler system. However, according to our best knowledge, there is no published  
13 data about the using of BSG/GTR mixture as low-cost hybrid reinforcement in  
14 biocomposites based on the elastomeric matrix.

## 15 16 **2. Experimental**

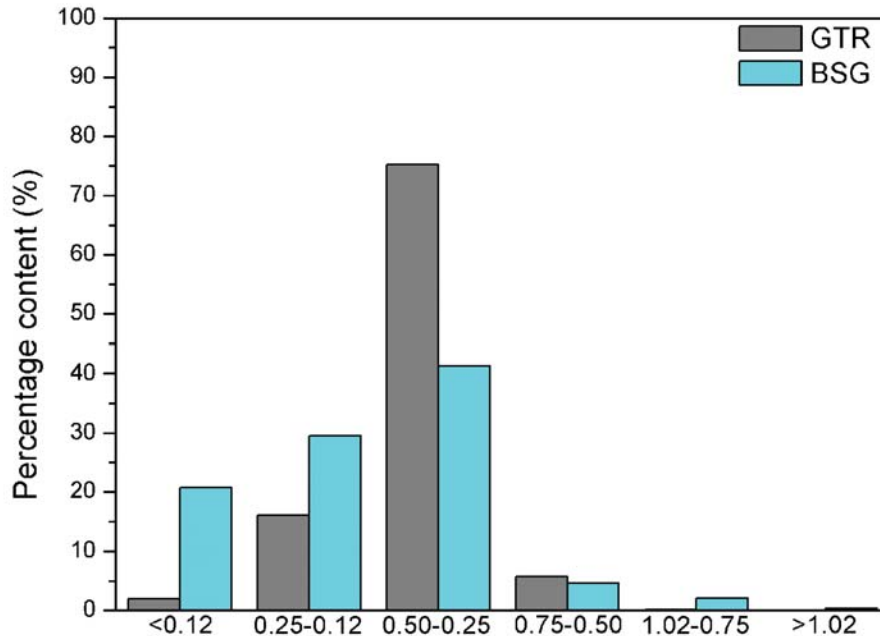
### 17 **2.1. Materials**

18 Natural rubber (NR) type RSS with density 0.92 g/cm<sup>3</sup> was supplied by Guma-  
19 Pomorska (Poland).

20 Ground tire rubber (GTR) with particles size below 0.8 mm was received from  
21 Orzeł S.A. (Poland). GTR was obtained during ambient grinding of used tires (mix of  
22 passenger car tires and truck tires). Prior to biocomposites preparation, GTR was  
23 mechano-chemically reclaimed at ambient temperature, in order to enhance matrix-filler  
24 interactions [22, 23]. For this purpose, GTR and 10 phr of modified bitumen Modbit  
25 25/55-60 were masticated for 10 minutes in small gap (less than 0.2 mm) using two-roll  
26 mills from Buzuluk (Czech Republic).

27 BSG was provided by home brewery Dno Bojlera (Poland). It was a by-product  
28 from the production of Christmas Ale and its initial composition contained (wt.%):  
29 3.7% chocolate wheat malt; 3.7% Special B malt; 6.7% Biscuit malt; 6.7% Carawheat  
30 malt; 19.4% pilsner malt; 22.4% Munich malt type II and 37.3% pale wheat malt.  
31 Almost half of malts (47.7 wt.%) were wheat malts, while the rest (52.3 wt.%) were  
32 barley malts. Prior to processing, BSG was dried at 80 °C and then mechanically

1 grounded in a co-rotating twin-screw extruder at 120 °C to obtain particles with a  
2 narrow size distribution. For better results analysis the particle size distribution of GTR  
3 and BSG is shown in Figure 1.



4  
5 Figure 1 Particle size distribution of GTR and BSG

6 Curing system components (TBBS - N-tert-butyl-2-benzothiazole sulfonamide,  
7 TMTD - tetramethylthiuram disulfide, stearic acid, zinc oxide and sulfur) with technical  
8 grade purity were supplied by Standard Sp. z o.o. (Poland).

## 9 10 2.2. Sample preparation

11 Highly filled biocomposites were prepared at 70 °C using a Brabender batch  
12 mixer model GMF 106/2 (Germany). The rotational speed of rotors was 100 rpm. The  
13 mixing time equaled 8 minutes which included 2 minutes of preliminary plasticization  
14 of natural rubber, 4 minutes of mixing with the 100 phr of waste filler (BSG, GTR or  
15 their mixture in variable ratio) and 2 minutes of mixing the blend with the sulfur curing  
16 system. For all samples the same curing system was used with composition (phr): zinc  
17 oxide 5.0; stearic acid 3.0; TBBS 1.0; TMTD 0.25; sulfur 2.0. After compounding in a  
18 batch mixer, the prepared biocomposites were homogenized using laboratory two roll  
19 mills from Buzuluk (Czech Republic). The obtained composites were compression  
20 molded into 2-mm thick samples at 160 °C and 4.9 MPa according to determined  
21 optimal cure time.

### 2.3. Measurements

Curing characteristics was investigated according to ISO 3417 at 160 °C, using Monsanto R100S rheometer with the oscillating rotor (USA). The rotor oscillation angle was 1°, while torque ranged between 0 and 100 dNm. Cure rate index (CRI) values were calculated in accordance with the formula (1):

$$\text{CRI} = \frac{100}{t_{90} - t_2} \quad (1)$$

where:  $t_{90}$  – optimum vulcanization time, min;  $t_2$  – scorch time, min.

The aging resistance of biocomposites at elevated temperatures was determined using a  $R_{300}$  parameter [24], which is the percentage reversion degree after a period of 300 s calculated from the time of reaching maximum torque value.  $R_{300}$  was calculated in accordance with the formula (2):

$$R_{300} = \frac{M_H - M_{300s}}{M_H} \times 100 \% \quad (2)$$

where:  $M_H$  – maximum torque;  $M_{300s}$  – torque 300 s after maximum torque.

Chemical structure of highly filled biocomposites was determined using Fourier transform infrared spectroscopy (FTIR) analysis performed by means of a Nicolet iS10 spectrometer from Thermo Scientific (USA). The device had an ATR attachment with a germanium crystal. Measurements were performed in a reflective absorbance mode (ATR-FTIR), at 1 cm<sup>-1</sup> resolution in the range 4000-650 cm<sup>-1</sup>.

The morphology of highly-filled biocomposites surfaces created by breaking the samples in the tensile test at the speed of 500 mm/min was observed with a JEOL 5610 scanning electron microscope (Japan). Before measurement, the samples were covered with a fine gold-palladium layer in order to increase their conductivity in a vacuum chamber.

Acoustic properties had been measured using a two-microphone impedance tube Brüel and Kjaer type 4206 in the frequency range 100–6500 Hz, according to ISO 10534-2, which describes the test method for impedance and absorption of acoustical materials using a tube, two microphones and a digital frequency analysis system.

1 Thermogravimetric analysis (TGA) was performed on a Mettler Toledo  
2 TGA/SDTA 851 apparatus (USA). NR-based composites weighing approx. 10-mg were  
3 placed in a corundum dish. The measurement was conducted in the temperature range  
4 50-650 °C and under a nitrogen atmosphere, at a heating rate of 20 °C/min.

5 Tensile strength and elongation at break of the obtained samples were tested  
6 according to the standard ISO 37 using a Zwick Z020 testing machine (Germany) with  
7 a load capacity of 20 kN. Tensile tests were performed at a cross-head speed of 500  
8 mm/min. Direct extension measurements were conducted periodically using an  
9 extensometer with sensor arms. Hardness was determined using a Zwick 3130  
10 durometer Shore A (Germany) in accordance with the standard ISO 7619-1. The  
11 reported results of tensile tests and hardness are the means of at least 5 measurements  
12 per sample.

13 Swelling degree of biocomposites (0.2 g samples) as a function of time was  
14 determined by equilibrium swelling in toluene (room temperature). Swelling degree was  
15 calculated in accordance with the formula (3):

$$16 \quad Q = \frac{m_t - m_o}{m_o} \times 100\% \quad (3)$$

17 where:  $Q$  – swelling degree, %;  $m_t$  – mass of the sample swollen after time  $t$ , g;  $m_o$  –  
18 initial mass of sample, g.

19 Cross-link density of the biocomposites was determined by equilibrium swelling  
20 in toluene (room temperature, 72 h), according to the Flory-Rehner equation [25] (4):

$$21 \quad v_e = \frac{-[\ln(1 - V_r) + V_r + \chi V_r^2]}{[V_1(V_r^{1/3} - V_r/2)]} \quad (4)$$

22 where:

23  $v_e$  – cross-link density, mol/cm<sup>3</sup>;  $V_r$  – gel volume in the swollen sample;  $V_1$  – solvent  
24 molar volume (toluene = 106.2, cm<sup>3</sup>/mol);  $\chi$  – polymer-solvent interaction parameter  
25 (in the calculations, it was assumed to be 0.393 [26]).

26 The Flory-Rehner equation can be applied for non-filled compounds, while  
27 studied samples contain cellulosic fillers. Kraus correction for filled compounds [27]  
28 was applied in order to calculate the actual remaining cross-link density. Cross-link  
29 density with Kraus correction was calculated according to equations (5) and (6):

$$30 \quad v_{\text{after correction}} = \frac{v_e}{1 + K \times \Phi} \quad (5)$$

$$\Phi = \frac{\phi_f \times \rho_r \times m_0}{\rho_f \times m_{dry}} \quad (6)$$

where:

$v_e$  – the measured chemical cross-link density, mol/cm<sup>3</sup>;  $v_{\text{after correction}}$  – the actual chemical cross-link density, mol/cm<sup>3</sup>; K – constant characteristic of the filler but independent of the solvent;  $\phi_f$  – the volume fraction of filler in the sample which is calculated;  $\rho_r$  – the density of studied compound, g/cm<sup>3</sup>;  $m_0$  – the weight of sample before extraction, g;  $\rho_f$  – the density of filler, g/cm<sup>3</sup>;  $m_{\text{dry}}$  – the weight of sample after extraction, g

Sol fraction was determined as the mass difference of biocomposites before swelling ( $W_1$ ) and after extraction ( $W_2$ ), according to equation (7):

$$\text{Sol fraction} = \frac{W_1 - W_2}{W_1} \times 100 \% \quad (7)$$

The density of the samples was measured based on the Archimedes method, as described in ISO 2781. Accordingly, all measurements were carried out at room temperature in methanol medium.

### 3. Results and discussion

#### 3.1. Curing characteristics

The effect of waste filler type (BSG, GTR or their mixture in variable ratio) on curing characteristics of highly filled NR-based composites is presented in Figure 2 and summarized in Table 1. It was observed that application of BSG/rGTR hybrid filler in ratio 75/25 resulted in an increase of minimal torque ( $M_L$ ) for 2.6 dNm, comparing to 1.7 dNm determined for NR/BSG composites. On the other hand, higher content of rGTR in studied composites had a negligible impact on this parameter, which was in the range 4.8-5.5 dNm. This indicates that application of 25 phr (and higher amount) of rGTR into biocomposites slightly deteriorating their further processing. This is due to the partially cross-linked structure of rGTR and carbon black present in this component. Additionally, BSG filler was characterized by smaller particles size comparing to GTR, which also affect the processing of studied biocomposites.

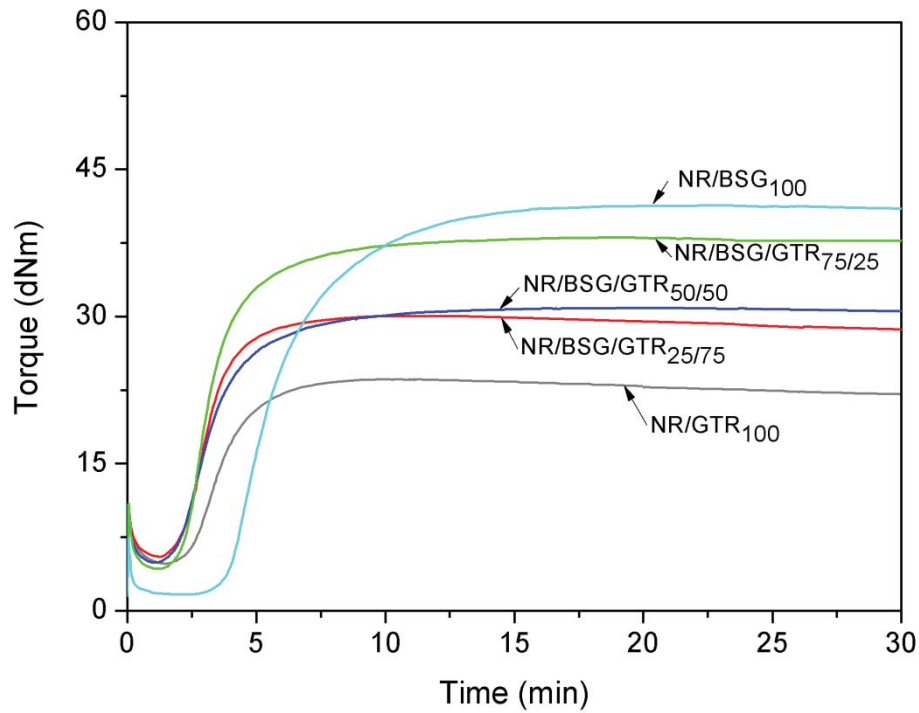
Maximal torque and torque increment ( $\Delta M = M_H - M_L$ ) values decreased with increasing content of GTR in biocomposites. This phenomenon is due to limited



1 mobility of polymer chains resulting from matrix-filler interactions and cross-link  
2 density, which have a significant impact on stiffness and shear modulus of  
3 biocomposites. The lowest and the highest torque values were determined for NR/BSG  
4 composite. This is related to the obvious difference in the chemical structure of used  
5 waste fillers. BSG is cellulosic filler with a high content (~20 wt.%) of proteins [28],  
6 which could act like plasticizers improving processing of rubber composites [29]. On  
7 the other hand, GTR is composed of natural rubber, synthetic rubbers, carbon black,  
8 curing system and other additives. It is worth to notice, that elastomers present in GTR  
9 possess unsaturated bonds, therefore during the preparation of biocomposites natural  
10 rubber matrix and GTR competed for curing agents. This phenomenon affects final  
11 cross-link density and stiffness of studied biocomposites.

12         It was observed, that regardless of GTR content, the addition of this filler caused  
13 a decrease of scorch time ( $t_2$ ) to 2.0-2.6 min, comparing to 3.9 min for the sample  
14 NR/BSG. This confirms that unreacted accelerators or other curing additives present in  
15 GTR migrate to natural rubber matrix during processing of biocomposites, which  
16 accelerate cross-link reaction upon heating and decrease scorch time [30]. A similar  
17 tendency was observed for optimal cure time ( $t_{90}$ ) and cure rate index (CRI) parameters.  
18 It was found that application of GTR to NR/BSG composites enhance their curing  
19 process, which resulted in a decrease of  $t_{90}$  and simultaneously increase of CRI. For  
20 example, optimum cure time for NR/BSG<sub>100</sub> was 10.1 min, while the addition of 25 phr  
21 GTR in NR/BSG/GTR<sub>75/25</sub> sample resulted in significant decreased of  $t_{90}$  to 6.0 min.  
22 This corresponded with an increase of cure rate index from 16.1 to 25.4 min<sup>-1</sup> for  
23 mentioned samples. Some minor differences in  $t_{90}$  and CRI parameters between sample  
24 NR/BSG/GTR<sub>75/25</sub> and NR/GTR<sub>100</sub> can be related to the complex structure of post-  
25 consumer GTR and presence of protein plasticizers in BSG, which might affect matrix-  
26 filler interactions and consequently curing characteristics. Additionally, it was observed  
27 that higher content of GTR in studied biocomposites resulted in their slightly lower  
28 thermal aging resistance, which could be due to their cross-link density.





1

2 Figure 2. Curing curves for highly-filled NR/BSG/GTR composites

3

4

Table 1. Composition and curing characteristics of studied biocomposites

Component (phr)*	Sample code				
	NR/BSG <sub>100</sub>	NR/BSG/GTR <sub>75/25</sub>	NR/BSG/GTR <sub>50/50</sub>	NR/BSG/GTR <sub>25/75</sub>	NR/GTR <sub>100</sub>
NR	100	100	100	100	100
BSG	100	75	50	25	0
rGTR	0	25	50	75	100
Curing characteristics at 160°C					
M <sub>L</sub> (dNm)	1.7	4.3	5.0	5.5	4.8
M <sub>H</sub> (dNm)	41.3	38.1	30.9	30.0	23.6
ΔM (dNm)	39.6	33.8	25.9	24.5	18.8
t <sub>2</sub> (min)	3.9	2.1	2.0	2.1	2.6
t <sub>90</sub> (min)	10.1	6.0	6.4	4.9	5.7
CRI (min <sup>-1</sup> )	16.1	25.4	22.5	35.3	31.8
R <sub>300</sub> (%)	0.5	0.8	0.6	0.5	1.1

5

\*For all samples the same curing system was used with composition (phr): zinc oxide 5.0; stearic acid 3.0; TBBS 1.0; TMTD 0.25; sulfur 2.0.

6

7

8

9

10

11

12

1  
2  
3  
4  
5  
6  
7  
8  
9  
10  
11  
12  
13  
14  
15  
16  
17  
18  
19  
20  
21  
22  
23  
24  
25  
26  
27

### 3.2. Fourier transform infrared spectroscopy analysis

FTIR spectra of NR-based composites modified with BSG/GTR hybrid fillers are presented in Figure 3. The small absorption band at  $3360\text{ cm}^{-1}$  (a) is attributed to O-H stretching vibrations. With increasing content of BSG the signal loses its intensity indicating the presence of OH groups mainly in GTR [31]. It may indicate that material undergoes degradation during processing. The bands in the range of  $2960\text{-}2850\text{ cm}^{-1}$  (b, c and d) are associated with the  $\text{CH}_3$  end-groups and symmetric and asymmetric stretching vibrations of C-H bonds in  $\text{CH}_2$  groups present in aliphatic elastomer chains. Absorption bands at  $1750$  and  $1660\text{ cm}^{-1}$  (e and f) are attributed to the stretching vibrations of C=O bonds and unconjugated C=C present in vulcanized natural rubber. Moreover, in the spectra of blends with BSG the intensity of those signals are different than for sample with GTR due to the presence of the same bonds in the cellulosic filler [32]. The absorption maxima at  $1540\text{ cm}^{-1}$  (g) can be related to the presence of zinc stearate formed during rubber compounding. An absorption maximum at  $1450\text{ cm}^{-1}$  (h) is attributed to the scissor vibrations of C-H bonds in  $\text{CH}_2$  groups of aliphatic chains of NR. The signal at  $1380\text{ cm}^{-1}$  (i) is associated with C-H bonds in  $\text{CH}_3$  end groups. The absorption band at  $1310\text{ cm}^{-1}$  (j) can be correlated with OH groups plane deformation vibrations. The band at  $1260\text{ cm}^{-1}$  (k) and signals at the range of  $1120\text{ - }1010\text{ cm}^{-1}$  (l, m and n) can be associated with vibrations of C-O, C-O-C, C-C-O and C=C groups present in BSG. In this range absorption maximum of  $\text{SiO}_2$ , present in GTR, can be found either. Those two facts explain the presence of the signals in all samples. The absorption band at  $806\text{ cm}^{-1}$  (o) is correlated with the bending vibrations of C-H in aliphatic chains of elastomer. The FTIR analysis demonstrated that type of used waste filler has a negligible influence on the chemical structure of the obtained NR based composites, which indicates mostly physical interactions between matrix and filler phase.

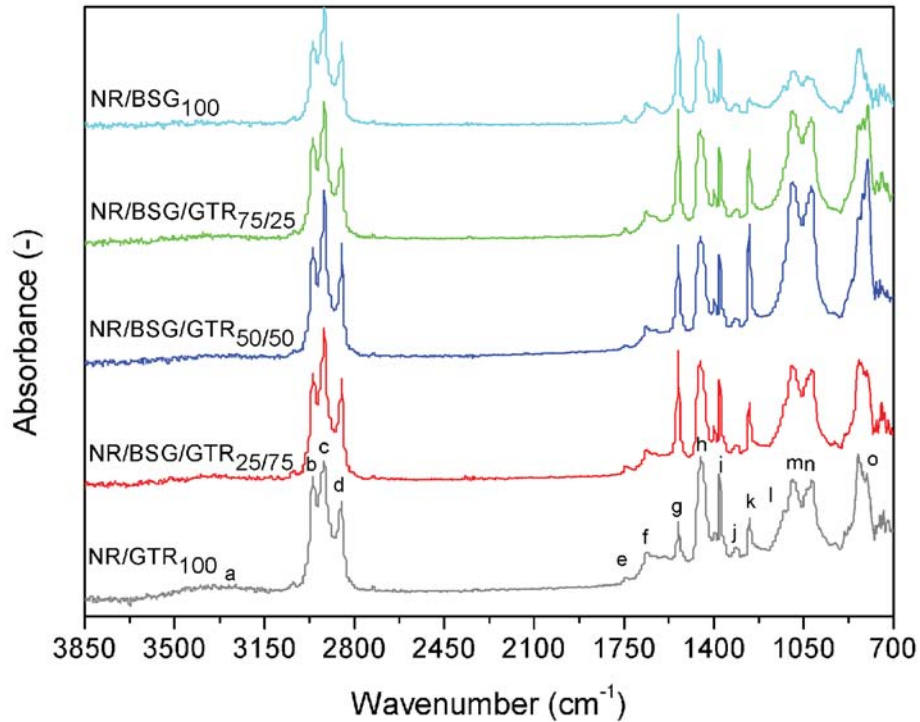


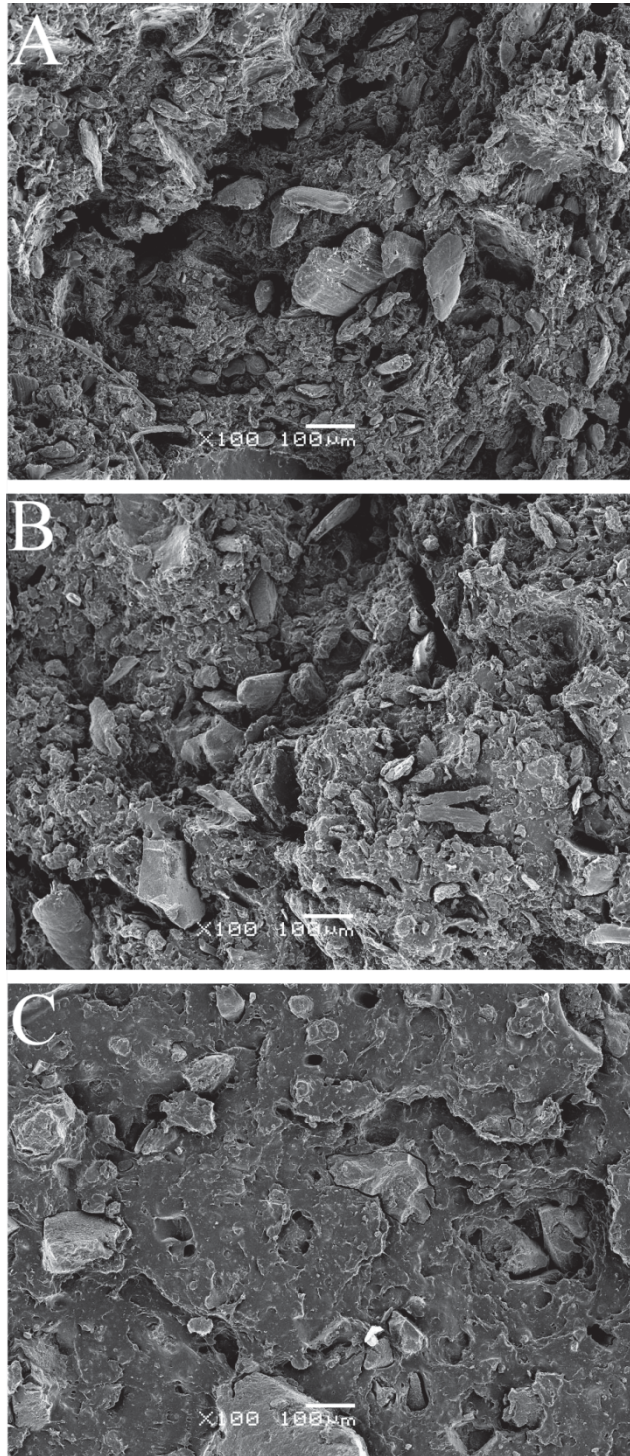
Figure 3. FTIR spectra for NR/BSG/GTR composites

### 3.3. Scanning electron microscopy

The impact of waste filler type on the morphology of biocomposites is presented in Figure 4. SEM images show the surface area perpendicular to the direction of strain, which was created by breaking of samples subjected to a static tensile test (cross-head speed was 500 mm/min). As could be observed in Figure 4A, the morphology of NR/BSG<sub>100</sub> sample is rough, while BSG filler is poorly dispersed into NR matrix. Moreover, BSG is surrounded by the gaps and voids what indicates weak compatibility between NR and BSG phases. This is related to the significant difference in polarity of used components, where NR is a hydrophobic matrix and BSG is hydrophilic filler. It was observed that homogeneity of NR/BSG/GTR<sub>50/50</sub> (Figure 4B) and NR/GTR<sub>100</sub> (Figure 4C) samples increased with higher content of GTR filler, which proved the higher interface interactions between NR matrix and GTR filler. On the micrographs showing the structure of NR/GTR blend (Figure 4C) single GTR grains and porous are visible while the most of it is homogenous.

This is due to the similar polarity of NR and GTR, which improves compatibility of studied systems. On the other hand, it is worth to mention about possible migration of components between natural rubber matrix and GTR (e.g. curing system, carbon black,

1 etc.), which can affect on co-vulcanization efficiency between the elastomeric matrix  
2 and GTR filler phase [33-34]. As a result, the NR matrix is able to transfer efficiently  
3 the applied loads to the reinforcing phase and enhancement of tensile properties is  
4 observed (see Physico-mechanical section).



5  
6 Figure 4. SEM images of samples: A – NR/BSG<sub>100</sub>, B – NR/BSG/GTR<sub>50/50</sub> and  
7 C – NR/GTR<sub>100</sub> (magnification x100)  
8



### 3.4. Physico-mechanical properties

The physico-mechanical properties are presented in Table 2. It was observed that with the increasing content of GTR tensile strength increases (NR/BSG<sub>100</sub> – 4.5 MPa, NR/BSG/GTR<sub>75/25</sub> – 5.8 MPa, NR/BSG/GTR<sub>50/50</sub> – 6.2 MPa, NR/BSG/GTR<sub>25/75</sub> – 7.8 MPa and NR/GTR<sub>100</sub> – 8.0 MPa, respectively). The similar trend is kept for elongation at break values (NR/BSG<sub>100</sub> – 475 %, NR/BSG/GTR<sub>75/25</sub> – 458 %, NR/BSG/GTR<sub>50/50</sub> – 491 %, NR/BSG/GTR<sub>25/75</sub> – 514 % and NR/GTR<sub>100</sub> – 511 %, respectively). As could be noticed, the addition of 75 phr of GTR filler significantly enhances mechanical properties of NR/BSG composite. NR has a tendency to strain-induced crystallization during tensile tests. Therefore, incorporation of fillers into NR matrix, can cause immobilization of polymer chains and disturb strain-induced crystallization process. This was proven with modulus at 100 % values which increase with higher content of BSG filler in studied samples. The analysis of mechanical properties shows that GTR has higher affinity to NR matrix than BSG due to the structure of waste tire rubber (composed mainly from natural rubber, synthetic rubber and carbon black). For better results presentation in Figure 5 strain-stress curves are presented for samples NR/BSG<sub>100</sub>, NR/BSG/GTR<sub>50/50</sub> and NR/GTR<sub>100</sub>. As could be expected, above mentioned limited chain mobility strongly influenced the hardness of tested samples. It was found that the addition of GTR caused hardness decrease (66, 61, 53, 49, 44 °Sh A for NR filled with BSG/GTR in ratio 100/0, 75/25, 50/50, 25/75, 0/100, respectively). The same decreasing trend is visible for the density of the samples. It is related to the constant amount sulfur curing system with increasing amount of GTR (which structure and properties are correlated with the amount of curing system).

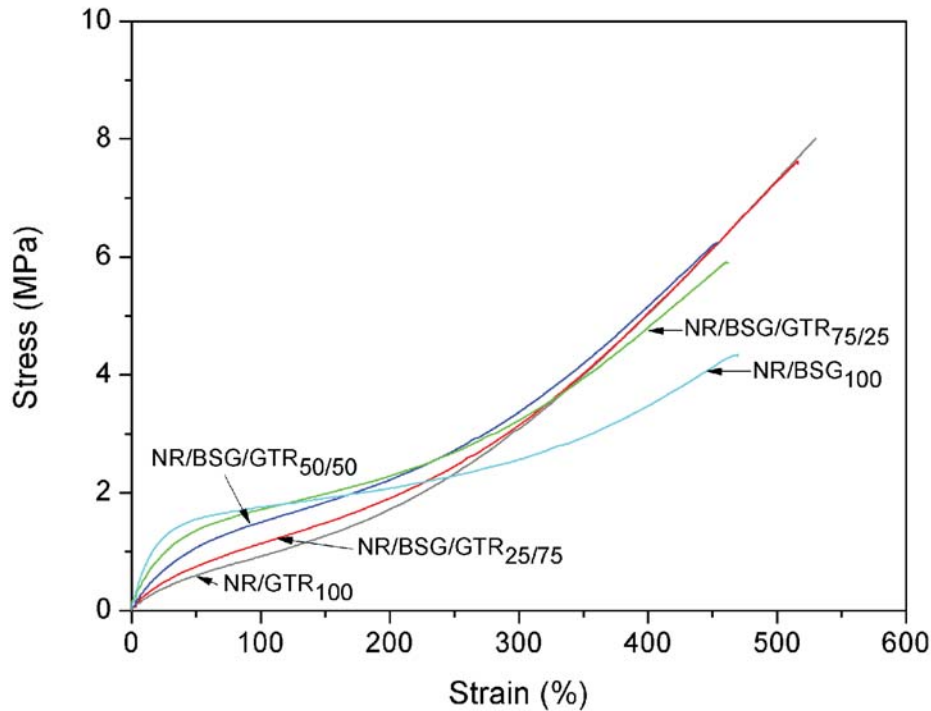
For a better understanding of the changes occurring in the structure of NR/BSG/GTR composites - sol fraction, swelling degree and cross-link density analysis were carried out. It was noticed that with higher content of GTR in NR/BSG composites the sol fraction values increases from 3.4 % for NR/BSG<sub>100</sub> to 6.5 % for NR/BSG/GTR<sub>25/75</sub> (7.6 % for NR/GTR<sub>100</sub> sample). This indicates that low molecular compounds present in GTR (e.g. organic non-polymeric ingredients and soluble rubber, etc.) are drawn out during extraction of NR/BSG/GTR composites [35]. Moreover, as mentioned in previous section NR matrix competed for cross-linking agents against GTR, which contain unsaturated bonds able for co-vulcanization in natural rubber. This

1 phenomenon corresponds with an increase of swelling degree and decrease of cross-link  
 2 density for NR/BSG/GTR composites with higher content of GTR filler due to the  
 3 constant amount of curatives.

4

5 Table 2. Physico-mechanical properties of NR-based composites

Item	NR/BSG <sub>100</sub>	NR/BSG/GTR <sub>75/25</sub>	NR/BSG/GTR <sub>50/50</sub>	NR/BSG/GTR <sub>25/75</sub>	NR/GTR <sub>100</sub>
Tensile strength (MPa)	4.5±0.1	5.8±0.2	6.2±1.4	7.8±0.4	8.0±0.4
Elongation at break (%)	475±12	458±16	491±31	514±16	511±27
Modulus at 100 %(MPa)	1.8±0.1	1.7±0.1	1.5±0.2	1.1±0.3	0.9±0.1
Hardness (°Sh A)	66	61	53	49	44
Density at 25°C (g/cm <sup>3</sup> )	1.11	1.09	1.08	1.06	1.04
Sol fraction (%)	3.4±0.2	4.4±0.2	5.3±0.2	6.5±0.2	7.6±0.2
Swelling degree (%)	232±2	226±2	228±6	257±6	277±4
Cross-link density (mol/cm <sup>3</sup> × 10 <sup>-4</sup> )	1.80±0.03	0.81±0.02	0.87±0.02	0.71±0.03	0.62±0.01



6

7 Figure 5. Stress-strain curves for studied NR/BSG/GTR composites

8

### 9 3.5. Acoustic properties

10 Application of lignocellulosic fillers, waste rubber and their mixture as low-cost  
 11 and efficient fillers for production of vibration and sound absorbers is a very promising  
 12 approach to their utilization [36-38]. The sound absorption coefficient ( $\alpha$ ) is defined as

1 the ratio of energy absorbed by the sample ( $E_a$ ) to the total energy incident acting on the  
2 sample energy ( $E_i$ ) on sample [39], as presented in equal (8):

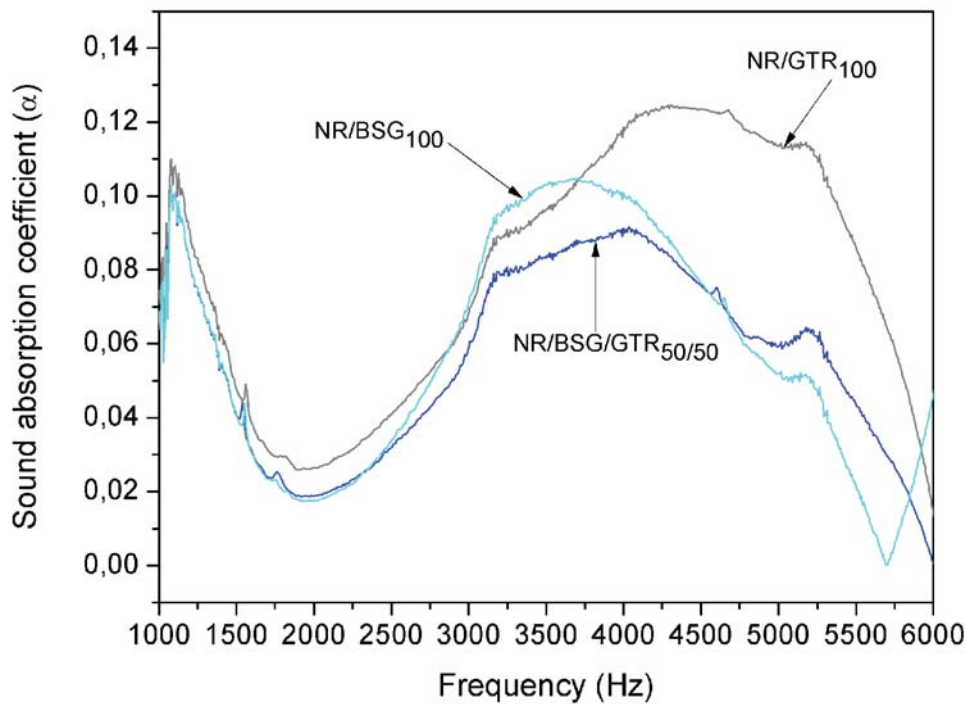
$$3 \quad \alpha = \frac{E_a}{E_i} = 1 - \left( \frac{n-1}{n+1} \right)^2 \quad (8)$$

4 Where  $n$  parameter is correlated to the ratio between measured maximum ( $p_{\max}$ ) and  
5 minimum ( $p_{\min}$ ) sound pressure inside the tube, as showed in equal (9):

$$6 \quad n = \frac{p_{\max}}{p_{\min}} \quad (9)$$

7 The relationships between sound absorption coefficients for NR/BSG/GTR  
8 composites and sound frequencies ranging from 1000 Hz to 6000 Hz are presented in  
9 Figure 6. It can be seen that at the frequency near 1000 Hz all samples characterize with  
10 the similar sound absorption. It was found that in the 3000-5500 Hz frequency range,  
11 NR/GTR<sub>100</sub> composite has higher sound absorption coefficient than NR/BSG<sub>100</sub> or  
12 NR/BSG/GTR<sub>50/50</sub> composites. This is due to the higher total content of carbon black in  
13 this sample. Zhao et al. [40] indicate that carbon black particles present in waste rubber  
14 act as barriers to sound waves. This phenomenon results in increasing diffraction and  
15 dispersion of the transmitted sound waves and consequently enhance acoustic properties  
16 of NR/GTR<sub>100</sub> sample. On the other hand, sound absorption coefficient curves for  
17 NR/BSG<sub>100</sub> and NR/BSG/GTR<sub>50/50</sub> composites showed a similar trend, while some  
18 minor differences can be due to the presence of voids and gaps in the structure, which  
19 strongly affect acoustic properties [41-42]. These observation corresponded to SEM  
20 microstructure analysis (see Figure 4) and density measurements (see Table 2).

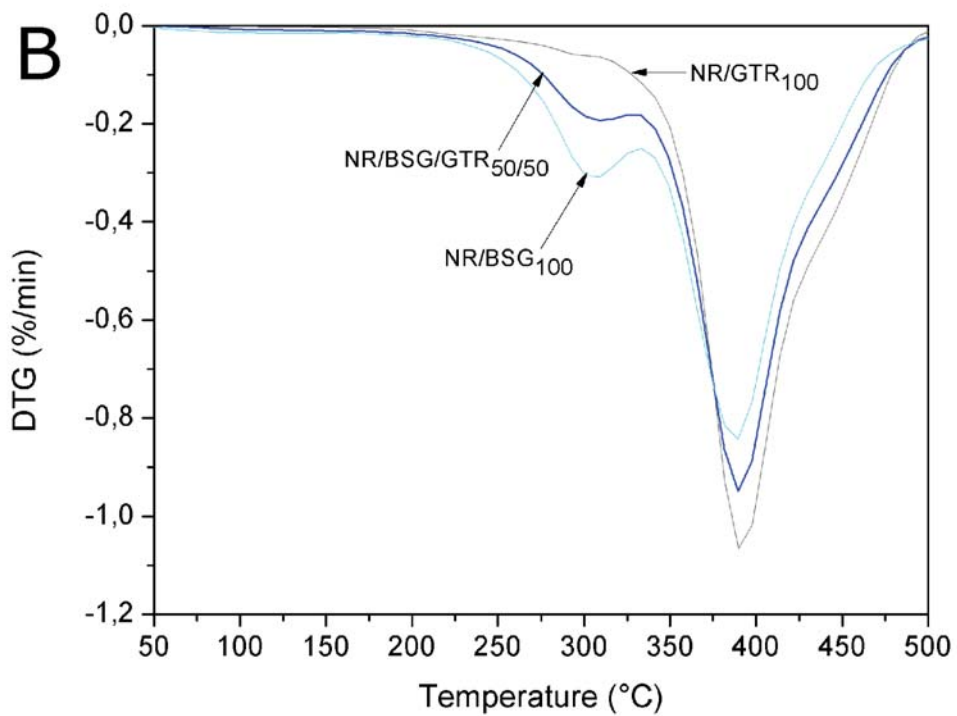
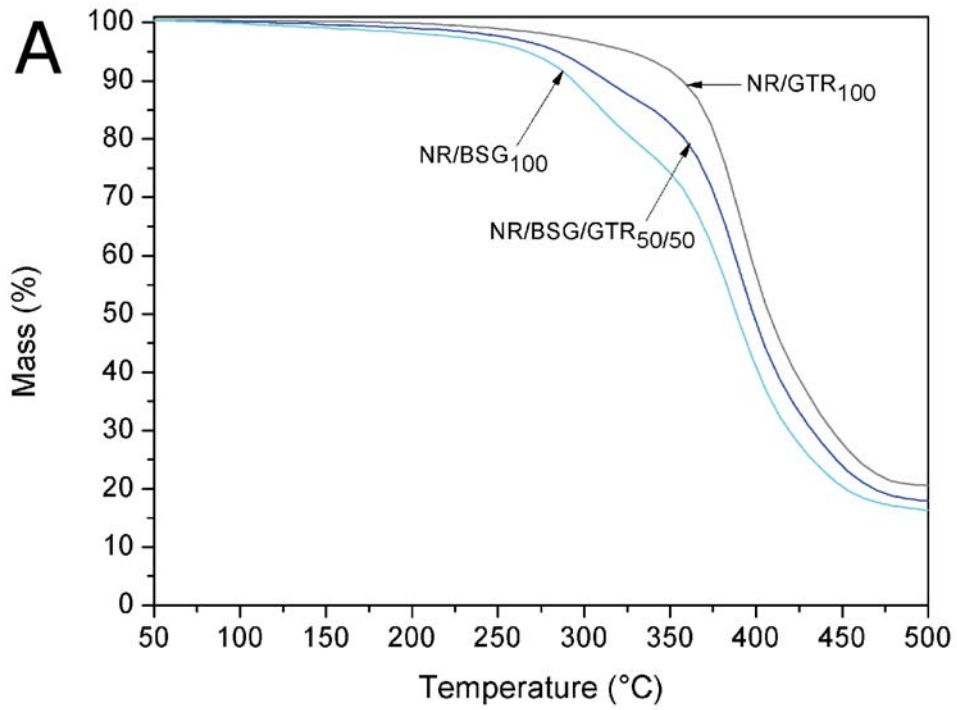




1  
2 Figure 6. Sound absorption coefficient as function of frequency for NR/BSG/GTR  
3 composites

### 5 3.6. Thermogravimetric analysis

6 The results of the thermogravimetric analysis of NR/GTR, NR/BSG/GTR and  
7 NR/BSG composites are presented in Figure 7 and summarized in Table 3. It can be  
8 assumed that increasing content of GTR caused an increase of the thermal stability. This  
9 phenomenon is due to the poor thermal stability of applied BSG in comparison to NR  
10 and GTR. As it could be predicted, with increasing content of GTR the decomposition  
11 of final products starts later. Moreover, the char residue is higher for samples containing  
12 GTR. This is due to the presence of carbon black and silica in applied waste tire  
13 rubber[43]. The first derivative of the TGA curves (the DTG curves) shows three main  
14 peaks. The first one at 309°C is correlated with thermal decomposition of cellulose and  
15 hemicellulose present in BSG filler [44]. The second peak at 390°C can be associated  
16 with decomposition of NR. The size of this signal is correlated with the amount of NR  
17 in the tested sample. Due to the presence of NR in GTR the peak for samples with a  
18 higher amount of GTR have higher intensity. Furthermore, for NR/GTR<sub>100</sub> and  
19 NR/BSG/GTR<sub>50/50</sub> samples third peak appears around 445°C which is associated with  
20 SBR [45].



1  
2  
3  
4  
5  
6  
7

Figure 7. A – TGA curves and B – DTG results for NR/BSG/GTR composites

1 Table 3. Thermal decomposition characteristics of studied composites

Sample	Mass loss (%)				Char residue at 650°C (%)
	2	5	10	50	
	Temperature (°C)				
NR/BSG <sub>100</sub>	210.7	267.5	295.1	388.9	15.7
NR/BSG/GTR <sub>50/50</sub>	243.9	286.1	314.2	398.7	17.5
NR/GTR <sub>100</sub>	279.5	326.8	357.7	407.8	20.4

2

3 **4. Conclusions**

4 Natural rubber (NR) composites highly filled with brewers' spent grain/ground tire  
 5 rubber (BSG/GTR) hybrid reinforcement were prepared in an batch mixer and followed  
 6 by cross-linking in hydraulic press. Curing characteristics, chemical structure, physico-  
 7 mechanical, thermal, morphological and acoustical properties of NR/BSG/GTR  
 8 composites were investigated as function of BSG/GTR ratio (in range: 100/0, 75/25,  
 9 50/50, 25/75 and 0/100 phr). It was observed that higher content of GTR in  
 10 NR/BSG/GTR composites accelerate cross-linking reactions during their preparation,  
 11 while simultaneously caused slight deterioration of samples processing. FTIR analysis  
 12 confirmed that interactions between NR matrix and hybrid BSG/GTR fillers were  
 13 mainly physical and have negligible effect on the chemical structure of NR/BSG/GTR  
 14 composites. Natural rubber matrix showed higher compatibility with GTR than with  
 15 BSG reinforcement phase, which was confirmed by the results of tensile tests, swelling  
 16 behavior, impedance tube measurements, TGA and SEM analysis. This is related to  
 17 differences in particles size and chemical structure of GTR and BSG, which have strong  
 18 impact on physical interactions and interfacial adhesion between NR matrix and  
 19 BSG/GTR hybrid reinforcement. Additionally, it was found that performance properties  
 20 of NR/BSG/GTR composites are also affected by migration of curing additives and  
 21 carbon black particles from GTR phase to NR matrix. This work confirms that  
 22 BSG/GTR hybrid fillers act as reinforcement phase into NR matrix, while the final  
 23 properties of composites can be successfully tailored by variable BSG/GTR ratio.

24

25

26

27

28

## 1 **References**

- 2 1. Karger-Kocsis J, Mészáros L, Bárány T. Ground tyre rubber (GTR) in thermoplastics,  
3 thermosets, and rubbers. *J Mater Sci* 2013;48(1):1-38.
- 4 2. Isikgor FH, Becer CR. Lignocellulosic biomass: a sustainable platform for the production  
5 of bio-based chemicals and polymers. *Polym Chem* 2015; 25(6):4497-4559.
- 6 3. Singh N, Hui D, Singh R, Ahuja IPS, Feo L, Fraternali F. Recycling of plastic solid  
7 waste: A state of art review and future applications, *Compos Part B-Eng* 2017;115:409-  
8 422.
- 9 4. Faruk O, Błędzki AK, Fink P, Sain M. Biocomposites reinforced with natural fibers:  
10 2000–2010. *Prog Polym Sci* 2012;37(11):1552-1596.
- 11 5. Sobczak L, Brüggemann O, Putz RF. Polyolefin composites with natural fibers and  
12 wood-modification of the fiber/filler–matrix interaction. *J Appl Polym Sci* 2013;127(1):  
13 1-17.
- 14 6. Zhou Y, Fan M, Che L, Zhuang J. Lignocellulosic fibre mediated rubber composites:  
15 An overview. *Compos Part B-Eng* 2015;76:180-191.
- 16 7. Zhou Y, Fan M, Chen L. Interface and bonding mechanisms of plant fibre composites.  
17 *Compos Part B-Eng* 2016;101:31-45.
- 18 8. Pickering KL, Aruan Efendy MG, Le TM. A review of recent developments in  
19 natural fibre composites and their mechanical performance, *Compos Part A-Appl S*  
20 2016;83:98-112.
- 21 9. Le Moigne N, Sonnier R, El Hage R, Rouif S. Radiation-induced modifications in  
22 natural fibres and their biocomposites: Opportunities for controlled physico-chemical  
23 modification pathways?. *Ind Crop Prod* 2017;109:199-213.
- 24 10. Gallos A, Paes G, Allais F, Beaugran J. Lignocellulosic fibers: A critical review of  
25 the extrusion process for enhancement of the properties of natural fiber composites.  
26 *RSC Adv.* 2017;55(7):34638-34654.
- 27 11. Formela K, Zedler Ł, Hejna A, Tercjak A, Reactive extrusion of bio-based polymer  
28 blends and composites – current trends and future developments. *Exp Polym Lett* 2018;  
29 12(1):24-57.
- 30 12. Attharangsarn S, Ismail H, Bakar MA, Ismail J. Carbon black (CB)/rice husk powder  
31 (RHP) hybrid filler-filled natural rubber composites: Effect of CB/RHP ratio on  
32 property of the composites. *Polym-Plast Technol* 2012;51(7):655-662.

- 1 13. Ahmed K, Nizami SS, Riza NZ. Reinforcement of natural rubber hybrid composites  
2 based on marble sludge/Silica and marble sludge/rice husk derived silica. *J Adv Res*  
3 2014;5(2):165-173.
- 4 14. Grzabka-Zasadzińska A, Klapiszewski Ł, Bula K, Jesionowski T, Borysiak S,  
5 Supermolecular structure and nucleation ability of polylactide-based composites with  
6 silica/lignin hybrid fillers. *J Therm Anal Calorim* 2016;126(1):263-275.
- 7 15. Abdul Salim ZAS, Hassan A, Ismail H. A review on hybrid fillers in rubber  
8 composites, *Polym-Plast Technol* 2017, doi: 10.1080/03602559.2017.1329432.
- 9 16. Kakroodi AR, Leduc S, Gonzalez-Nunez R, Rodrigue D. Mechanical properties of  
10 recycled polypropylene/SBR rubber crumbs blends reinforced by birch wood flour.  
11 *Polym Polym Compos* 2012;20(5):439-444.
- 12 17. Kakroodi AR, Rodrigue D. Impact modification of polypropylene-based composites  
13 using surface-coated waste rubber crumbs. *Polym Compos* 2014;35(11):2280-2289.
- 14 18. Kakroodi AR, Kazemi Y, Rodrigue D. Mechanical, rheological, morphological and  
15 water absorption properties of maleated polyethylene/hemp composites: Effect of  
16 ground tire rubber addition. *Compos Part B-Eng* 2013;51:337-344.
- 17 19. Kakroodi AR, Rodrigue D. Reinforcement of maleated polyethylene/ground tire  
18 rubber thermoplastic elastomers using talc and wood flour. *J Appl Polym Sci*  
19 2014;131(8): 40195.
- 20 20. Nikpour N, Rodrigue D. Effect of coupling agent and ground tire rubber content on  
21 the properties of natural fiber polymer composites. *Int Polym Proc* 2016;31(4):463-471.
- 22 21. Formela K, Hejna A, Zedler Ł, Ryl J, Saeb MR, Piszczyk Ł. Structural, thermal and  
23 physico-mechanical properties of polyurethane/brewers' spent grain composite foams  
24 modified with ground tire rubber. *Ind Crop Prod* 2017;108C:844-852.
- 25 22. Li S, Lamminmäki J, Hanhi K. Improvement of mechanical properties of rubber  
26 compounds using waste rubber/virgin rubber. *Polym Eng Sci* 2005; 45:1239-1246.
- 27 23. Formela K, Cysewska M, Haponiuk J, Thermomechanical reclaiming of ground tire  
28 rubber via extrusion at low temperature: Efficiency and limits. *J Vinyl Addit Techn*  
29 2016;22:213-221.
- 30 24. Khang TH, Ariff ZM. Vulcanization kinetics study of natural rubber compounds  
31 having different formulation variables. *J Therm Anal Calorim* 2012;109(3):1545-1553.

- 1 25. Flory PJ, Rehner J. Statistical mechanics of cross-linked polymer networks I.  
2 rubberlike elasticity. *J Chem Phys* 1943;11:512-520.
- 3 26. López-Manchado MA, Herrero B, Arroyo M. Preparation and characterization of  
4 organoclay nanocomposites based on natural rubber. *Polym. Int* 2003;52:1070–1077.
- 5 27. Kraus GJ. Swelling of filler-reinforced vulcanizates. *J Appl Polym Sci* 1963;7:861-  
6 871.
- 7 28. Öztürk S, Özboy Ö, Cavidoğlu İ, Köksel H. Effects of brewer's spent grain on the  
8 quality and dietary fibre content of cookies *J. Inst. Brew* 2002;108:23-27.
- 9 29. Karaağaç B. Use of ground pistachio shell as alternative filler in natural  
10 rubber/styrene-butadiene rubber-based rubber compounds. *Polym Compos*  
11 2014;35:245–252.
- 12 30. Sreeja TD, Kutty SKN. Studies on acrylonitrile butadiene rubber/reclaimed rubber  
13 blends. *J Elastomers Plast* 2002;34:145–155.
- 14 31. Zhang X, Lu C, Liang M. Properties of natural rubber vulcanizates containing  
15 mechanochemically devulcanized ground tire rubber. *J Polym Res* 2009;16:411-419.
- 16 32. Gunasekaran S, Natarajan RK, Kala A. FTIR spectra and mechanical strength  
17 analysis of some selected rubber derivatives. *Spectrochim Acta Part A Mol Biomol*  
18 *Spectrosc* 2007;68:323–330.
- 19 33, Gibala D, Hamed GR. Cure and mechanical behavior of rubber compounds  
20 containing ground vulcanizates. Part I: cure behavior. *Rubber Chem Technol*  
21 1994;67:636–648.
- 22 34. Formela K, Haponiuk J. Curing characteristics, mechanical properties and  
23 morphology of butyl rubber filled with ground tire rubber (GTR). *Iran Polym J*  
24 2014;23:185.
- 25 35. Zhang X, Lu Z, Tian D, Li H, Lu C. Mechanochemical devulcanization of ground  
26 tire rubber and its application in acoustic absorbent polyurethane foamed composites. *J*  
27 *Appl Polym Sci* 2013;127:4006–4014.
- 28 36. Zhu X, Kim BJ, Wang Q, Wu Q. Recent advances in the sound insulation properties  
29 of bio-based materials. *BioResources* 2014;9:1764-1786.
- 30 37. Karger-Kocsis J. Waste tyre rubber – what to do next?. *Express Polym Lett* 2013;7:  
31 406.

- 1 38. Yang H, Kim D, Lee Y, Kim H, Jeon J, Kang C. Possibility of using waste tire  
2 composites reinforced with rice straw as construction materials. *Bioresour Technol*  
3 2004;95:61-65.
- 4 39. Markiewicz E, Borysiak S, Paukszta D. Polypropylene-lignocellulosic material  
5 composites as promising sound absorbing materials. *Polimery* 2009;54:430-435.
- 6 40. Zhao J, Wang XM, Chang JM, Yao Y, Cui Q. Sound insulation property of wood-  
7 waste tire rubber composite. *Compo Sci Technol* 2010;70:2033-2038.
- 8 41. Colom X, Cañavate J, Carrillo F, Lis M. Acoustic and mechanical properties of  
9 recycled polyvinyl chloride/ground tyre rubber composites. *J Compos Mater*  
10 2014;48:1061–1069.
- 11 42. Ubaidillah, Harjana, Yahya I, Kristiani R, Muqowi E, Mazan SA. Perfect sound  
12 insulation property of reclaimed waste tire rubber, *AIP Conference Proceedings*,  
13 2016;1717(1):050012.
- 14 43. Seidelt S, Müller-Hagedorn M, Bockhorn H. Description of tire pyrolysis by  
15 thermal degradation behaviour of main components. *J Anal Appl Pyrolysis* 2006;75:11–  
16 18.
- 17 44. Prins MJ, Ptasinski KJ, Janssen FJ. Torrefaction of wood: Part 1. Weight loss  
18 kinetics. *J Anal Appl Pyrol* 2006;77:28–34.
- 19 45. Garcia PS, de Sousa FDB, de Lima JA, Cruz SA, Scuracchio CH. Devulcanization  
20 of ground tire rubber: Physical and chemical changes after different microwave  
21 exposure times. *Express Polym Lett* 2015;9:1015–1026.

22

23

24

25

26

27

28

29



1 **Tables and Figures captions**

2 Table 1. Composition and curing characteristics of studied biocomposites

3 Table 2. Physico-mechanical properties of NR-based composites

4 Table 3. Thermal decomposition characteristics of studied composites

5

6 Figure 2 Particle size distribution of GTR and BSG

7 Figure 2. Curing curves for highly-filled NR/BSG/GTR composites

8 Figure 3. FTIR spectra for NR/BSG/GTR composites

9 Figure 4. SEM images of samples: A – NR/BSG<sub>100</sub>, B – NR/BSG/GTR<sub>50/50</sub> and  
10 C – NR/GTR<sub>100</sub> (magnification x100)

11 Figure 5. Stress-strain curves for studied NR/BSG/GTR composites

12 Figure 6. Sound absorption coefficient as function of frequency for NR/BSG/GTR  
13 composites

14 Figure 7. A – TGA curves and B – DTG results for NR/BSG/GTR composites

15

16